Neuropharmacology 102 (2016) 80–91

Contents lists available at ScienceDirect

Neuropharmacology

journal homepage: www.elsevier.com/locate/neuropharm

Pharmacological kynurenine 3-monooxygenase enzyme inhibition significantly reduces neuropathic pain in a rat model

Ewelina Rojewska, Anna Piotrowska, Wioletta Makuch, Barbara Przewlocka, Joanna Mika*

Department of Pain Pharmacology, Institute of Pharmacology, Polish Academy of Sciences, 12 Smetna Street, 31-343 Krakow, Poland

ARTICLE INFO

Article history:
Received 23 July 2015
Received in revised form
17 October 2015
Accepted 27 October 2015
Available online 31 October 2015

Keywords:
Chronic constriction injury (CCI)
IL-6
IL-1beta
NOS2
Kynurenine 3-monooxygenase
Minocycline

ABSTRACT

Recent studies have highlighted the involvement of the kynurenine pathway in the pathology of neurodegenerative diseases, but the role of this system in neuropathic pain requires further extensive research. Therefore, the aim of our study was to examine the role of kynurenine 3-monooxygenase (Kmo), an enzyme that is important in this pathway, in a rat model of neuropathy after chronic constriction injury (CCI) to the sciatic nerve. For the first time, we demonstrated that the injury-induced increase in the *Kmo* mRNA levels in the spinal cord and the dorsal root ganglia (DRG) was reduced by chronic administration of the microglial inhibitor minocycline and that this effect paralleled a decrease in the intensity of neuropathy. Further, minocycline administration alleviated the lipopolysaccharide (LPS)-induced upregulation of *Kmo* mRNA expression in microglial cell cultures. Moreover, we demonstrated that not only indirect inhibition of Kmo using minocycline but also direct inhibition using Kmo inhibitors (Ro61-6048 and JM6) decreased neuropathic pain intensity on the third and the seventh days after CCI. Chronic Ro61-6048 administration diminished the protein levels of IBA-1, IL-6, IL-1beta and NOS2 in the spinal cord and/or the DRG. Both Kmo inhibitors potentiated the analgesic properties of morphine. In summary, our data suggest that in neuropathic pain model, inhibiting Kmo function significantly reduces pain symptoms and enhances the effectiveness of morphine. The results of our studies show that the kynurenine pathway is an important mediator of neuropathic pain pathology and indicate that Kmo represents a novel pharmacological target for the treatment of neuropathy.

1. Introduction

The involvement of the kynurenine system in the pathology of neurodegenerative diseases (i.e., Huntington's disease, migraines and multiple sclerosis) has been demonstrated, but the importance of this pathway in neuropathic pain is poorly understood and requires extensive research. Recently, Wilson et al. (2014) stressed that kynurenine 3-monooxygenase (Kmo), a member of the kynurenine pathway, is a particularly important enzyme in neurodegeneration. Kmo facilitates the formation of anthranilic acid, 3-hydroxyanthranilic acid and 3-hydroxykynurenine, and these successive processes lead to an increase in the level of quinolinic acid (QUIN). QUIN is a selective, endogenous N-methyl-D-aspartate (NMDA) receptor agonist that contributes to neurodegenerative processes (Behan and Stone, 2000; Schwarcz et al., 2012). It is well known that NMDA receptor antagonists relieve neuropathic pain (Collins et al., 2010). Therefore, QUIN, as the final product of Kmo activity, is highly likely to affect neuropathic pain. Previous studies have shown that Ro61-8048, a Kmo inhibitor, displays neuroprotective activity in models of cerebral hypoxia (Moroni et al., 2005). Moreover, Zwilling et al. (2011) have shown that Kmo inhibitors (Ro61-8048 and JM6) exerted similar therapeutic effects in mouse models of Huntington's and Alzheimer's diseases; however comparable studies of nociceptive transmission are lacking.

In our recently published studies using microarray methods, we showed for the first time that upregulation of the *Kmo* gene paralleled that of a microglial activation marker during neuropathic pain. Moreover, we showed in these models that intraperitoneal (*i.p.*) administration of minocycline (a microglial inhibitor) decreased pain and *Kmo* mRNA expression in the spinal cord (Rojewska et al., 2014b). Interestingly, the kynurenine pathway has previously been shown to be predominantly active in macrophages and microglia (Guillemin et al., 2003). These cells play a crucial role in the development of allodynia and hyperalgesia in animal models

* Corresponding author. Institute of Pharmacology, Polish Academy of Sciences, Department of Pain Pharmacology, 12 Smetna St., 31-343 Krakow, Poland.
E-mail addresses: joamika@if-pan.krakow.pl, joasia272@onet.eu (J. Mika).

http://dx.doi.org/10.1016/j.neuropharm.2015.10.040
0028-3908/

of neuropathic pain (Milligan and Watkins, 2009; Rojewska, 2014a,c; Mika et al., 2009, 2013). Minocycline inhibits microglial activation; consequently, it is able to downregulate proinflammatory factors (e.g., NOS2, IL-6 and IL-18) in the spinal cord and/or the dorsal root ganglia (DRG) (Rojewska et al., 2014c; Makuch et al., 2013).

It remains unclear how Kmo inhibitors influence the development of neuropathic pain. Therefore, our studies were designed to address this issue. Using qRT-PCR, we assessed how chronic *i.p.* or intrathecal (*i.t.*) administration of minocycline influenced the nerve injury-induced increase in the *Kmo* mRNA levels in the spinal cord and the DRG. Furthermore, we evaluated whether *i.t.* administration of the Kmo enzyme inhibitor Ro61-8048 or its prodrug JM6 influences pain development and the levels of glia-released pronociceptive factors (i.e., IL-1beta, IL-6 and NOS2) in a rat model of neuropathic pain. Moreover, we examined whether Kmo inhibitors (i.e., Ro61-6048 and JM6) influence the analgesic properties of morphine in this model. The objective of our *in vitro* studies was to determine whether the *Kmo* mRNA level changes in primary microglial or astroglial cell cultures treated with lipopolysaccharide (LPS) and how minocycline influences such changes.

2. Materials and methods

2.1. Animals

Our experiments were performed using male Wistar rats (weighing from 300 g to 350 g) from Charles River (Hamburg, Germany). The animals were housed in cages lined with sawdust under a 12-h dark/light cycle and were provided with free access to food and water. All efforts were made to minimize animal suffering and to reduce the number of animals used. All experiments followed the recommendations of the International Association of Studies on Pain (Zimmermann, 1983) and were approved by the Local Bioethics Committee of the Institute of Pharmacology (Krakow, Poland).

2.2. Intrathecal catheter placement

Rats were anesthetized via *i.p.* injection of pentobarbital (60 mg/kg), and their heads were fixed on a stereotaxic table (David Kopf Instruments, Tujunga, CA, USA). A surgical incision was made in the atlanto-occipital membrane according to the method of Yaksh and Rudy (1976). A 7.8-cm-long catheter (PE 10; Intramedic; Clay Adams; Becton, Dickinson and Company; Rutherford, NJ, USA) was slowly introduced into the subarachnoid space of the spinal cord to the lumbar enlargement (L4–L5). After placement, the catheters were slowly flushed with sterile water and closed.

2.3. Neuropathic pain model (chronic constriction injury, CCI)

Five days after the intrathecal catheter insertion, CCI was performed according to the method of Bennett and Xie (1988). The operation was performed under sodium pentobarbital anesthesia (60 mg/kg; *i.p.*). Four ligatures (4-0 silk) were tied loosely around the nerve of the right hind paw distal to the sciatic notch with 1-mm intervals between the ligatures. After surgery, all animals developed sustained allodynia and hyperalgesia in the injured hind paw.

2.4. Drug administration

The following substances were used: minocycline hydrochloride (Sigma, Schnelldorf, Germany), Ro61-8048 (Tocris, Janki/Warsaw, Poland) and JM6 (Merck Millipore, Warsaw, Poland). Before the drug injections, the baseline behaviors of the animals were determined using von Frey and cold plate tests. The behavioral tests were conducted 30 min after a single *i.t.* injection of Ro61-8048 or JM6 at a dose of 10, 20, 40, 80, or 120 μg. For the chronic treatment, the drugs were injected *i.t.* at the selected dose (20 μg for Ro61-8048 and JM6 or 60 μg for minocycline hydrochloride) according to the following scheme: preemptively 16 h and 1 h following CCI and then once daily for 7 days. This injection schedule is referred to as "repeated administration" throughout this article. Alternatively, minocycline hydrochloride (30 mg/kg; *i.p.*) was injected 16 h preceding and 1 h following CCI and then administered twice daily for 7 days. The doses and the schedule of minocycline administration were used as described previously (Mika et al., 2007; Rojewska et al., 2014c). The control groups received vehicle (injection of water or dimethyl sulfoxide, DMSO) according to the same schedule. For injection, minocycline hydrochloride was dissolved in water, and the Kmo inhibitors were dissolved in DMSO. All drugs were administered via *i.t.* injection of a volume of 5 μl, and the drug injections were followed by an injection of 10 μl of water to flush the catheter. The DMSO-treated, Ro61-8048-treated and JM6-treated rats received a single *i.t.* injection of morphine (10 μg/5 μl) on day 7 post-CCI, and 30 min afterward, the von Frey test and the cold plate test were repeated.

2.5. Behavioral tests

2.5.1. Tactile allodynia (von Frey test)

A von Frey apparatus (Dynamic Plantar Aesthesiometer, Cat. No. 37400, Ugo Basile, Varese, Italy) was used to assess mechanical allodynia. Five minutes before the experiment, each rat was placed in a plastic cage with a wire net floor to promote behavioral accommodation. The weight of the von Frey stimuli used in our experiments was up to 26 g. The mid-plantar ipsilateral and contralateral hind paw areas were tested, and measurements were recorded automatically as described previously (Makuch et al., 2013; Rojewska et al., 2014a). No significantly different contralateral hind paw reactions were observed between the rats subjected to CCI and the naive rats. Allodynia was assessed 30 min after the final drug administration.

2.5.2. Hyperalgesia (cold plate test)

Cold hyperalgesia was assessed using the cold plate test (Cold/Hot Plate Analgesia Meter, Cat. No. 05044, Columbus Instruments, Columbus, OH, USA) as previously described (Makuch et al., 2013; Mika et al., 2007). The rats were placed on a cold stainless steel plate maintained at 5 °C, and the latency to lift or shake the injured hind paw was measured. The cut-off latency was 30 s.

2.6. Microglial cell cultures and treatments

Primary cultures of microglia and astroglia were prepared from 1-day-old Wistar rats according to the procedure described by Zawadzka and Kaminska (2005). Cells were isolated from the cerebral cortex and then plated in a poly-L-lysine-coated 75 cm^2 culture flask at a density of 3×10^5 cells/cm^2 in high-glucose GlutaMax DMEM (Gibco, Grand Island, NY, USA) supplemented with 10% heat-inactivated fetal bovine serum, 0.1 mg/ml streptomycin and 100 U/ml penicillin (Gibco, Grand Island, NY, USA). The cultures were maintained at 37 °C in 5% CO_2. On the fourth day of culture, the culture medium was replaced. On the ninth day, the culture was gently shaken and centrifuged to recover the loosely adherent microglia. Then, the medium was replaced, and on the twelfth day, the microglia were recovered again. Once again, the culture medium was replaced, and the culture was gently shaken on a rotary shaker at 37 °C for 24 h (200 rpm) to remove the

remaining non-adherent cells. The medium was removed, and the resulting astrocytes were plated on culture plates and cultured for three days. Then, the astrocytes were trypsinized (0.005% trypsin EDTA solution, Sigma–Aldrich, Saint Louis, MO, USA). Microglia and astrocytes were seeded at a final density of 2×10^5 cells/perwell in 24-well plates for analysis of the mRNA levels in the cultures after incubation for 48 h. Primary microglial and astrocyte cell cultures were treated with minocycline (20 μM) for 30 min before administration of LPS (100 ng/ml) (Sigma–Aldrich, Saint Louis, MO, USA) for 24 h. To identify astrocytes *in vitro*, we stained the cultures for the astrocyte marker glial fibrillary acidic protein (GFAP; more than 95% of the cells were positive for GFAP; SC-166 458, Santa Cruz Biotechnology, Inc., Santa Cruz, CA, USA). Furthermore, to identify the microglia in the cultures, we stained for the microglial marker ionized calcium-binding adapter molecule 1 (IBA-1, more than 95% of the cells were positive for IBA-1; SC-327 225, Santa Cruz Biotechnology, Inc., Santa Cruz, CA, USA). The homogeneity of our cultures was similar to that reported by Zawadzka and Kaminska (2005).

2.7. Biochemical tests

2.7.1. Collection of tissues and cells for RNA isolation

Ipsilateral, dorsal lumbar spinal cord segments (L4–L6) and DRG (L4–L6) were collected for biochemical analysis on the 3rd, 7th or 14th day after CCI. After the final administration of chronic Ro61-8048 treatment on day 7 after CCI (4 h and 6 h after drug administration for quantitative reverse transcriptase polymerase chain reaction [qRT-PCR] and western blot analysis, respectively), the rats were decapitated, and tissue was collected. The samples were placed in individual tubes containing the tissue storage reagent RNAlater (Qiagen Inc., Valencia, CA, USA), frozen on dry ice, and stored at −70 °C until RNA extraction. Cell samples were collected using TRIzol reagent. Total RNA was extracted according to the method of Chomczynski and Sacchi (1987) with modifications using TRIzol reagent (Invitrogen).

According to the manufacturer's instructions, the RNA concentration was determined using a NanoDrop ND-1000 Spectrometer (NanoDrop Technologies), and the RNA quality was determined via chip-based capillary electrophoresis using an RNA 6000 Nano LabChip Kit and an Agilent 2100 Bioanalyzer (Agilent).

2.7.2. Quantitative reverse transcriptase polymerase chain reaction (qRT-PCR)

Reverse transcription (RT) was performed using 1000 ng of total RNA as a template along with Omniscript reverse transcriptase (Qiagen) and oligo(dT16) primers. The reactions were incubated at 37 °C for 60 min. RT reactions were performed in the presence of an RNase inhibitor (rRNAsin, Promega) and an oligo (dT16) primers (Qiagen, Inc.). cDNA was diluted 1:10 in H_2O. qRT-PCR was performed using Assay-On-Demand TaqMan probes according to the manufacturer's protocol (Applied Biosystems), and the procedures were conducted using an iCycler real-time PCR thermal cycler (Bio-Rad, Hercules, CA, USA). In our experiments, we used the following TaqMan primers and probes: Rn01423590_m1 (*CD40,* CD40 molecule), Mm01253033_m1 (*Gfap*, glial fibrillary acidic protein), Rn00580432_m1 (*IL-1beta*, interleukin 1 beta), Rn00561420_m1 (*IL-6,* interleukin 6), Rn00561646_m1 (*NOS2,* nitric oxide synthase 2), and Rn00665313_m1 (*Kmo,* kynurenine 3-monooxygenase). The threshold cycle values were calculated automatically by iCycler IQ 3.0a software using the default parameters. The abundance of RNA was calculated as $2^{-(\text{threshold cycle})}$. The expression of the hypoxanthine guanine phosphoribosyl transferase 1 (Hprt1 - Rn01527838_g1) transcript, which was stable following drug treatment, was calculated to relative to the control (naive) levels to account for variation in cDNA amounts. In previous studies, we demonstrated that the HPRT transcript levels do not significantly change in rats subjected to CCI (Mika et al., 2008; Rojewska et al., 2014a,b); thus, HPRT served as an adequate housekeeping gene.

2.7.3. Western blot

Tissue lysates were collected in RIPA buffer containing a protease inhibitor cocktail and were cleared via centrifugation (14,000 × g for 30 min at 4 °C). Samples containing 20 μg of protein were heated in loading buffer (50 mM Tris–HCl, 2% SDS, 2% β-mercaptoethanol, 4% glycerol and 0.1% bromophenol blue) for 5 min at 98 °C and were resolved on 10–20% or 4–20% Criterion™ TGX™ pre-cast polyacrylamide gels. Following gel electrophoresis, the proteins were transferred to Immun-Blot PVDF membranes (Bio-Rad) via semi-dry transfer (30 min, 25 V). The membranes were blocked for 1 h at room temperature using 5% non-fat dry milk (Bio-Rad) in Tris-buffered saline containing 0.1% Tween-20 (TBST), washed in TBST, and incubated overnight at 4 °C in primary antibodies (rabbit polyclonal anti-IBA-1 (Millipore); rabbit polyclonal anti-IL-1beta (Abcam), 1:1000; rabbit polyclonal anti-IL-6 (Invitrogen), 1:1000; rabbit polyclonal anti-NOS2 (Santa Cruz), 1:500; rabbit polyclonal anti-Kmo (Proteintech), 1:500; rabbit polyclonal anti-GFAP (Novus Biologicals), 1:5000; and mouse polyclonal anti-GAPDH (Millipore), 1:5000, as a loading control). Then, the membranes were incubated for 1 h in horseradish peroxidase-conjugated anti-rabbit or anti-mouse secondary antibodies. Both primary and secondary antibodies were diluted in solutions from the SignalBoost Immunoreaction Enhancer Kit (Merck Millipore). The membranes were washed 2 × 2 min and 3 × 5 min with TBST. Immunocomplexes were detected using an Immun-Star HRP Chemiluminescent Substrate Kit (BioRad) and were visualized using a Fujifilm LAS-4000 FluorImager system. The relative levels of immunoreactivity were quantified using Fujifilm MultiGauge software.

2.8. Immunocytochemistry

Morphological changes in microglia and astroglia were determined via immunocytochemistry using commercially available antibodies against IBA-1 and GFAP. Unstimulated and LPS-stimulated (for 24 h) microglia and astrocytes were cultured on sterile cover slips in 6-well plates (1×10^6 cells/well). The cells were fixed for 20 min in 4% paraformaldehyde (Sigma Aldrich, Saint Louis, MO, USA). Then, the cells were permeabilized with 0.1% Triton™ X-100 (Sigma Aldrich, Saint Louis, MO, USA) in PBS for 30 min at room temperature, washed with PBS and blocked with 5% goat serum in PBS. The microglial and astroglial cells were incubated in primary antibodies (rabbit anti-IBA-1 (Proteintech), 1:500, and mouse anti-GFAP (Santa Cruz Biotechnology, Inc.), 1:500, respectively) overnight at 4 °C. After washing with PBS, the microglia and the astroglia were incubated for 2–3 h in a fluorophore-conjugated secondary antibody: Alexa Fluor 555 goat anti-rabbit or Alexa Fluor 488 goat anti-mouse (Molecular Probes) diluted 1:500 in 5% normal donkey serum (NDS). Then, the cells were washed with PBS and coverslipped using Aquatex mounting medium (Merck, Darmstadt, Germany). Morphological changes after LPS administration were evaluated by visualizing microglia and astrocytes under the 40× objective of a Zeiss microscope (Zeiss, Germany).

2.9. Statistical analyses

The means ± SEM of the behavioral data are presented in grams or seconds, and each group, including the naive groups, contained

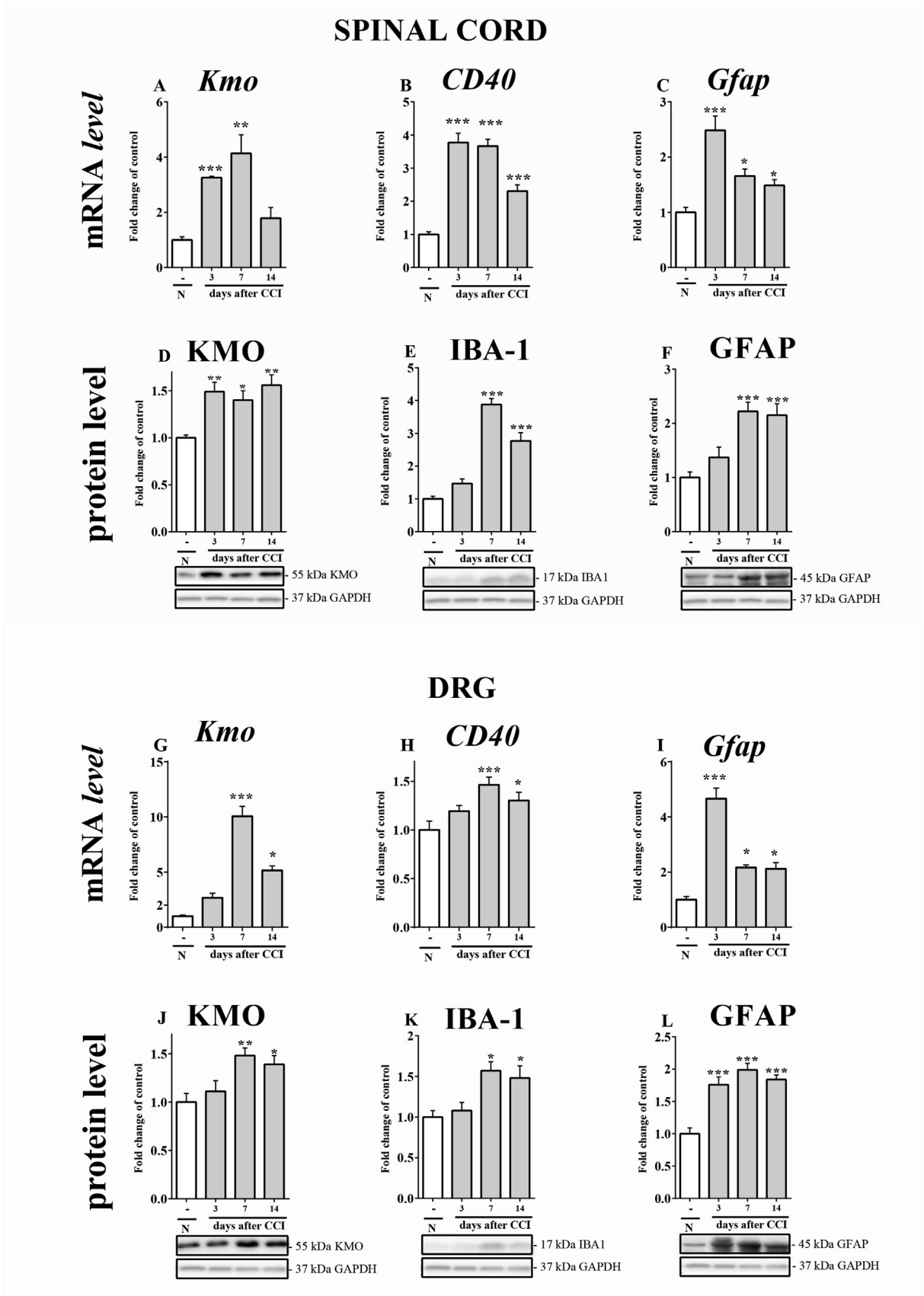

Fig. 1. qRT-PCR (A-C and G-I) and Western blot (D-F and J-L) analysis of the mRNA and protein levels of *Kmo* (A, D, G, J), *CD40*, *IBA-1* (B, E, H, K) and *Gfap* (C, F, I, L) in the ipsilateral dorsal spinal cord (L4-L6) and DRG (L4-L6) on days 3, 7 and 14 after CCI in rats. The data are shown as the mean fold-changes in expression relative to the control (naïve, N) levels ± SEM (4–9 samples per group). Inter-group differences were analyzed using Bonferroni's test for multiple comparisons. $^{*}p < 0.05$, $^{**}p < 0.01$, and $^{***}p < 0.001$ indicate significant differences compared to the naïve group.

6–14 rats. The inter-group differences were analyzed via one-way analysis of variance (ANOVA) followed by Bonferroni's test for multiple comparisons.

The results of qRT-PCR (Figs. 1, 3 and 5; 4–9 samples) and Western blot (Figs. 1 and 5; 4–7 samples) analyses are presented as fold-changes in expression relative to the levels in the control group (naive rats); these values were calculated for the ipsilateral spinal cords and DRG of the CCI-exposed rats. The qRT-PCR data are presented as the means ± SEM and represent the normalized averages derived from the threshold cycle obtained via qRT-PCR. The results of the experiments were evaluated via one-way ANOVA. The inter-group differences were analyzed via ANOVA followed by Bonferroni's test for multiple comparisons.

The results from the primary microglial and astroglial cultures are presented as the fold-change in expression relative to the levels in the control (vehicle-treated) group of non-stimulated cells. The data are presented as the means ± SEM. The inter-group differences were analyzed via ANOVA followed by Bonferroni's test for multiple comparisons.

All graphs were prepared using GraphPad Prism software (version 5.0).

3. Results

3.1. Changes in Kmo gene expression – in vivo and in vitro studies

3.1.1. Quantification of the mRNA and protein levels of KMO, CD40/IBA-1 and GFAP in the spinal cord and DRG over time after CCI

On days 3 and 7, strong, significant upregulation of *Kmo* mRNA expression (1 ± 0.1 *vs.* 3.3 ± 0.04 and 1 ± 0.1 *vs.* 4.13 ± 0.6, respectively) was observed in the spinal cord of rats subjected to CCI compared with naive rats. No change in *Kmo* mRNA expression in the spinal cord was observed on day 14 after CCI (Fig. 1A). CCI led to significant upregulation of *Kmo* mRNA in the DRG at 7 and 14 days after CCI (1 ± 0.1 *vs.* 10.1 ± 0.9 and 1 ± 0.1 vs. 5.15 ± 0.4, respectively) (Fig. 1G). Based on Western blot analysis, the protein level of KMO in the spinal cord was increased on days 3, 7 and 14 after CCI compared with naïve treatment (1 ± 0.03 *vs.* 1.5 ± 0.1, 1 ± 0.03 *vs.* 1.4 ± 0.1 and 1 ± 0.03 *vs.* 1.6 ± 0.1, respectively) (Fig. 1D). In the DRG (Fig. 1J), upregulation of the KMO protein was observed on days 7 and 14 after CCI (1 ± 0.1 *vs.* 1.5 ± 0.1 and 1 ± 0.1 *vs.* 1.4 ± 0.1, respectively).

The *CD40* mRNA level in the spinal cord was elevated after CCI at all examined time points. The following changes in *CD40* mRNA expression were found in the spinal cord on days 3, 7 and 14: 1 ± 0.07 *vs.* 3.7 ± 0.3, 1 ± 0.07 *vs.* 3.7 ± 0.2 and 1 ± 0.07 *vs.* 2.3 ± 0.2, respectively (Fig. 1B). In the DRG, upregulation of *CD40* mRNA was detected on days 7 and 14 after CCI relative to the *CD40* mRNA level after naive treatment (1 ± 0.1 *vs.* 1.5 ± 0.08 and 1 ± 0.1 *vs.* 1.3 ± 0.08, respectively) (Fig. 1H). An increase in IBA-1–positive cells was observed on days 7 and 14 in the spinal cord (1 ± 0.1 *vs.* 3.9 ± 0.2 and 1 ± 0.1 *vs.* 2.8 ± 0.2, respectively) (Fig. 1E) and in the DRG (1 ± 0.1 *vs.* 1.6 ± 0.1 and 1 ± 0.1 *vs.* 1.5 ± 0.1, respectively) of CCI-treated rats compared with naive rats (Fig. 1K).

In both the spinal cord and the DRG, the *Gfap* mRNA level was significantly increased on day 3 after CCI (1 ± 0.1 *vs.* 2.5 ± 0.2 and 1 ± 0.1 *vs.* 4.7 ± 0.4, respectively). Additionally, on days 7 and 14, the *Gfap* mRNA level was elevated (but was lower than the level on day 3) in both examined structures (Fig. 1C and I). At the protein level, we observed an increase in GFAP–positive cells after CCI compared with naïve treatment based on Western blot analysis (Fig. 1F and L). This increase in GFAP–positive cells was observed on days 7 and 14 after CCI in the spinal cord (1 ± 0.1 *vs.* 2.2 ± 0.2 and 1 ± 0.1 *vs.* 2.1 ± 0.2, respectively) (Fig. 1F) and on days 3, 7 and 14 after CCI in the DRG (1 ± 0.1 *vs.* 1.8 ± 0.1, 1 ± 0.1 *vs.* 2.0 ± 0.1 and 1 ± 0.1 *vs.* 1.8 ± 0.1, respectively) (Fig. 1L).

3.1.2. Study of minocycline influence of the Kmo expression in primary microglial and astroglial cell cultures

Our immunocytochemical analyses (Fig. 2A and C) demonstrated that the morphology of microglia was altered from a ramified (V/-, vehicle-treated non-stimulated) to an amoeboid appearance after treatment with LPS for 24 h. In astroglia, no changes in morphology were observed after LPS treatment (Fig. 2C). The *Kmo* mRNA levels were significantly increased in microglia at 24 h after LPS treatment (Fig. 2B). However, minocycline significantly reduced the *Kmo* mRNA levels in the primary microglial cultures after LPS stimulation. The *Kmo* mRNA level in astroglia was not affected by LPS or minocycline injection (Fig. 2D).

3.1.3. The influence of repeated i.t. or i.p. administration of minocycline on allodynia and Kmo mRNA expression in the spinal cord and the DRG on day 7 after CCI

In the von Frey test, strong allodynia in the paw ipsilateral to the injury was observed on day seven after CCI. At this time point, the ipsilateral paw responded to a stimulus of 11.0 ± 0.4 g, whereas naive rats first responded to a stimulus of 26.0 ± 0.7 g (Fig. 3A). Repeated *i.p.* administration of minocycline significantly attenuated this allodynia, as demonstrated by an increase in the response threshold from 12.04 ± 0.5 g to 17.1 ± 0.7 g (Fig. 3A). Furthermore, repeated *i.t.* administration of minocycline decreased allodynia in rats subjected to CCI, as demonstrated by an increase in the response threshold from 11.04 ± 0.4 g to 16.8 ± 0.4 g (Fig. 3D).

Repeated *i.p.* administration of minocycline significantly decreased the *Kmo* mRNA levels in the spinal cord (from 3.9 ± 0.5 to 1.4 ± 0.3) (Fig. 3B) and in the DRG (from 10.9 ± 1.20 to 4.4 ± 0.6) (Fig. 3C). Similar results were observed after *i.t.* administration of minocycline: minocycline attenuated the injury-induced increase in the *Kmo* mRNA level in the spinal cord and the DRG (from 4.9 ± 1.4 to 0.35 ± 0.2 and from 4.3 ± 0.9 to 0.9 ± 0.18, respectively) (Fig. 3E and F).

3.2. Behavioral and biochemical effects of inhibiting Kmo expression

3.2.1. The influence of a single i.t. administration of Ro61-8048 or JM6 at different doses on allodynia and hyperalgesia on day 7 after CCI

The effect of single *i.t.* administration of Ro61-8048 or JM6 (10 μg, 20 μg, 40 μg, 80 μg or 120 μg) was measured using von Frey and cold plate tests. Ro61-8048 at 20 μg, 40 μg, 80 μg and 120 μg decreased CCI-induced allodynia and hyperalgesia. Moreover, administration of JM6 at a dose of 40 μg, 80 μg or 120 μg reduced the symptoms of neuropathic pain after CCI, as demonstrated by the results on the cold plate test, and JM6 treatment at the highest doses reduced pain symptoms, as demonstrated by the results on the von Frey test, compared with vehicle treatment (Table 1).

3.2.2. The influence of repeated i.t. administration of the Kmo inhibitors Ro61-8048 and JM6 at selected doses on allodynia and hyperalgesia on days 3 and 7 after CCI

The effect of repeated administration of a Kmo inhibitor, i.e., Ro61-8048 or JM6 (both at a dose of 20 μg), was studied in CCI-treated rats (Fig. 4A and B). The naive animals reacted to the mechanical stimulus at a weight of 25.6 ± 0.2 g on the von Frey test and responded to low temperature after 29.15 ± 0.5 s on the cold plate test. After CCI, all rats exhibited strong allodynia in the paw ipsilateral to the injury (as demonstrated by the von Frey test results on days 3 and 7 after CCI: 12.4 ± 0.5 g and 14.9 ± 0.4 g, respectively) (Fig. 4A), and all rats exhibited potent hyperalgesia (as

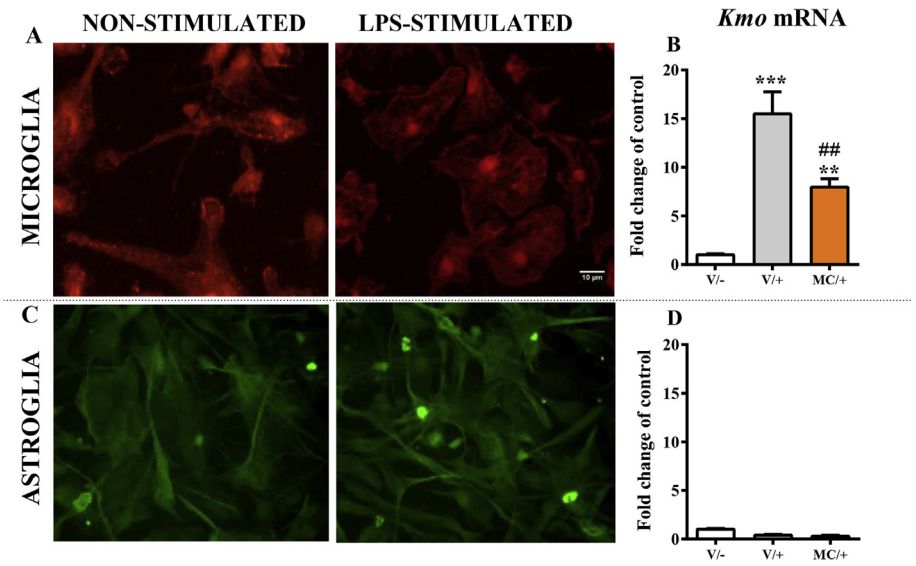

Fig. 2. Images of immunofluorescence staining for markers of microglia (IBA-1; A) and astroglia (GFAP; C) are presented. Primary microglial (B) and astroglial (D) cell cultures were treated with vehicle (V) or minocycline (MC; 20 μM) 30 min before the administration of lipopolysaccharide (LPS; 100 ng/μl). At 24 h after LPS stimulation, the *Kmo* mRNA level was analyzed. The qRT-PCR data are presented as the means ± SEM and represent the normalized averages from the analyses of three experiments. $^{**}p < 0.01$ and $^{***}p < 0.001$ indicate significant differences compared to non-stimulated cells (V/-); $\#\#p < 0.01$ indicates a significant difference between the **V/+** and **MC/+** groups. Abbreviations: **V/-** (control, V-treated non-stimulated cells); **V/+** (V-treated LPS-stimulated cells); **MC/+** (MC-treated LPS-stimulated cells). The scale bar for all microphotographs is 10 μm.

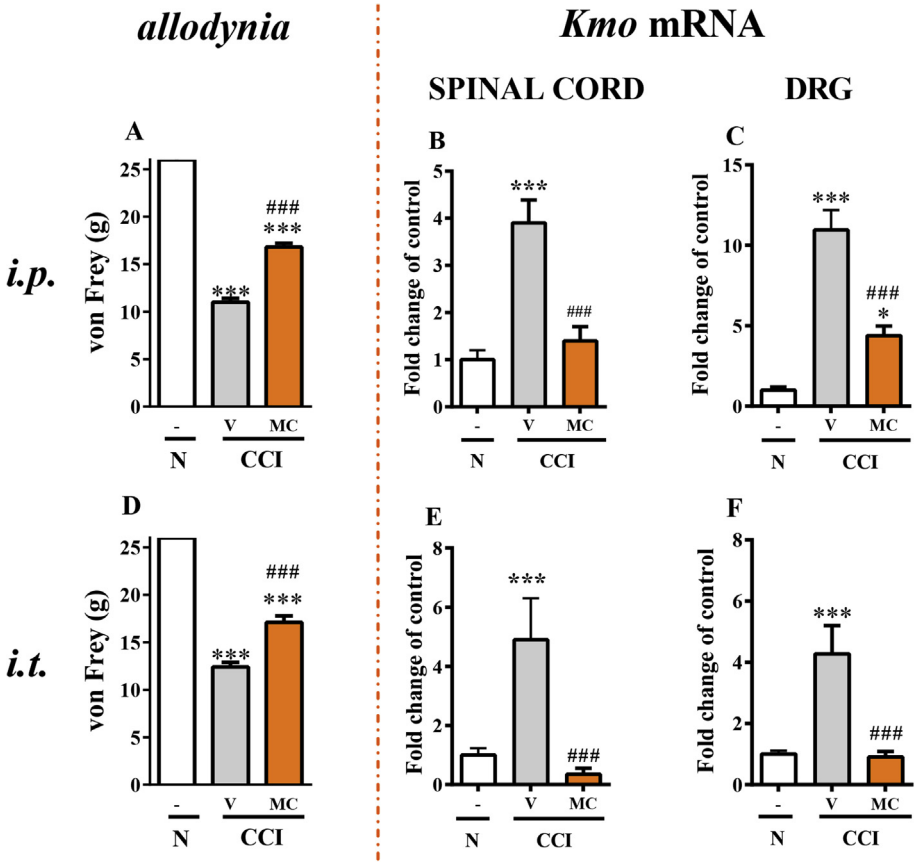

Fig. 3. Effects of repeated minocycline (MC) administration (A, 30 mg/kg *i.p.*; D, 60 μg *i.t.*) on allodynia (A, D) and on the mRNA levels of *Kmo* in the dorsal lumbar (L4–L6) spinal cord (B, E) and DRG (C, F) 7 days after CCI. The behavioral results are presented as the means ± SEM (8–14 rats per group). The biochemical data are presented as the mean fold-changes in expression relative to the control (naïve group) levels ± SEM (4–9 samples per group). Inter-group differences were analyzed via one-way ANOVA followed by Bonferroni's test for multiple comparisons. $^{***}p < 0.001$ indicates a difference compared to the naïve group; $\#\#\#p < 0.001$ indicates a difference compared to the V–CCI group. Abbreviations: N (naïve group); V–CCI (V-treated CCI-exposed group); MC-CCI (MC-treated CCI-exposed group).

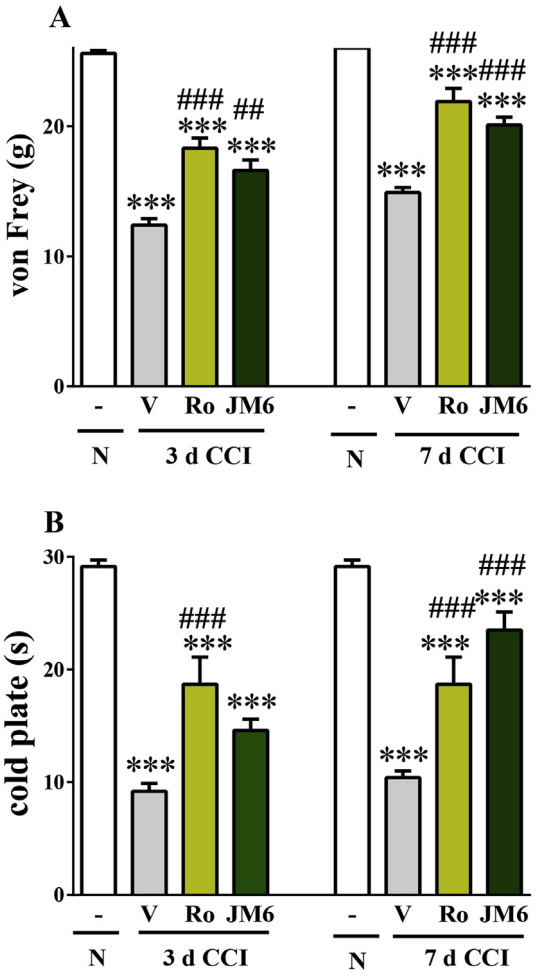

Fig. 4. The effect of *i.t.* administration of a Kmo inhibitor, either Ro61-8048 or JM6, at a dose of 20 μg on allodynia (von Frey test; A) and hyperalgesia (cold plate test; B) in rats on days 3 and 7 after CCI. Both Kmo inhibitors significantly reduced allodynia and hyperalgesia. The results are presented as the means ± SEM (6–14 rats per group). Inter-group differences were analyzed via one-way ANOVA followed by Bonferroni's test for multiple comparisons. ***$p < 0.001$ indicates a difference compared to the naïve group; ##$p < 0.01$ and ###$p < 0.001$ indicate differences compared to the V-treated CCI-exposed group. Abbreviations: N (naïve group); V–CCI (DMSO-treated CCI-exposed group); Ro (Ro61-8048-treated CCI-exposed group).

demonstrated by the response latency on the cold plate test: 9.2 ± 0.7 s and 10.4 ± 0.6 s, respectively (Fig. 4B). Both Ro61-8048 and JM6 diminished pain symptoms on day 3 after CCI (Fig. 4A and B). On day 7 after CCI, injection of Ro61-8048 or JM6 reduced allodynia (21.9 ± 1.0 g and 20.1 ± 0.6 g, respectively) and hyperalgesia (18.7 ± 2.4 s and 23.5 ± 1.6 s, respectively) (Fig. 4A and B).

3.2.3. The influence of repeated i.t. administration of Ro61-8048 on the CD-40, IL-6, IL-1beta and NOS2 mRNA and protein levels in the spinal cord and the DRG on day 7 after CCI

In rats subjected to CCI, *CD40* mRNA expression in the spinal cord was upregulated (1.0 ± 0.1 vs. 7.1 ± 0.3) compared with that in naive rats (Fig. 5A). Ro61-8048 decreased the relative level of *CD40* mRNA in the spinal cord after CCI from 7.1 ± 0.3 to 5.1 ± 0.3. Additionally, in the DRG, the *CD40* mRNA levels were significantly increased from 1.0 ± 0.01 in naïve rats to 9.1 ± 2.3 (Fig. 5I) in rats subjected to CCI. Similarly, Ro61-8048 significantly decreased the *CD40* mRNA levels in the DRG after CCI from 9.1 ± 2.3 to 2.9 ± 0.3 (Fig. 5I).

Based on Western blot analysis, in the spinal cord, IBA-1 protein was upregulated from 1.0 ± 0.05 in naïve animals to 3.0 ± 0.3 in CCI-treated animals (Fig. 5E). Ro61-8048 decreased the level of this microglial activation marker after CCI from 3.0 ± 0.28 to 2.2 ± 0.15 (Fig. 5E). In the DRG, the IBA-1 protein levels were significantly higher in CCI-treated rats than in naïve rats (2.7 ± 0.2 *vs.* 1.0 ± 0.1) (Fig. 5M). Ro61-8048 decreased the IBA-1 protein levels in the DRG after CCI from 2.7 ± 0.2 to 1.3 ± 0.1 (Fig. 5M).

The *IL-6* mRNA level in the spinal cord was strongly upregulated in CCI-treated rats compared with naive rats (31.2 ± 3.8 *vs.* 1 ± 0.2) (Fig. 5 B). Repeated treatment with Ro61-8048 significantly decreased the relative level of *IL-6* mRNA in the spinal cord after CCI from 31.2 ± 3.8 to 3.1 ± 1.6 (Fig. 5B). In the DRG, *IL-6* mRNA expression was upregulated in CCI rats compared with naive rats (186.7 ± 13.1 *vs.* 1 ± 0.07). Ro61-8048 significantly decreased the relative level of *IL-6* mRNA in the DRG after CCI from 186.7 ± 13.1 to 87.5 ± 15.9 (Fig. 5J).

The IL-6 protein level in the spinal cord was increased in CCI rats compared to naive animals (1.2 ± 0.5 *vs.* 1 ± 0.04). Chronic administration of Ro61-8048 reduced the IL-6 protein level in the spinal cord after CCI from 1.2 ± 0.5 to 1.0 ± 0.1 (Fig. 5F). Furthermore, the IL-6 protein level was upregulated in the DRG from 1.0 ± 0.1 after naïve treatment to 1.7 ± 0.06 after CCI (Fig. 5N). After Ro61-8048 injection, we observed a reduction in the protein level of IL-6 in the DRG (Fig. 5N).

The expression of *IL-1beta* mRNA was upregulated from 1.0 ± 0.09 to 45.6 ± 1.6 in the spinal cord (Fig. 5C) and from 1.0 ± 0.1 to 51.07 ± 10.8 in the DRG (Fig. 5K) in the CCI-treated rats relative to the naive rats. Ro61-8048 did not influence the mRNA levels of *IL-1beta* in the spinal cord, but Ro61-8048 significantly decreased the *IL-1beta* mRNA levels in the DRG after CCI from 51.07 ± 10.8 to 16.6 ± 3.4 (Fig. 5K).

Seven days after CCI, based on Western blot analysis, we detected an increased protein level of IL-1beta in the spinal cord (from 1.02 ± 0.02 to 1.25 ± 0.06) and in the DRG (from 1.02 ± 0.1 to 1.65 ± 0.2) relative to the IL-1beta protein levels after naive treatment (Fig. 5G and O). Ro61-8048 administration did not influence the protein levels of *IL-1beta* in the spinal cord (Fig. 5G) but did decrease the *IL-1beta* mRNA levels in the DRG after CCI from 1.65 ± 0.2 to 0.9 ± 0.04 (Fig. 5O).

The relative *NOS2* mRNA expression level was increased in the spinal cord from 1 ± 0.1 to 145.2 ± 19.3 (Fig. 5D) and in the DRG from 1 ± 0.4 to 2547.04 ± 736.7 in the CCI rats compared with the naive rats (Fig. 5L). Ro61-8048 decreased the relative levels of *NOS2* mRNA after CCI in the spinal cord from 145.2 ± 19.3 to 7.8 ± 0.9 and in the DRG from 2547.04 ± 736.7 to 64.55 ± 17.4 (Fig. 5D and L).

Based on Western blot analysis, in the spinal cord, NOS2 protein was upregulated from 1.0 ± 0.1 to 2.2 ± 0.1 in CCI-treated animals compared with naïve animals (Fig. 5H). Ro61-8048 decreased the level of NOS2 in the spinal cord after CCI from 2.2 ± 0.1 to 1.3 ± 0.2 (Fig. 5H). In the DRG, the NOS2 protein levels were higher in CCI-treated rats than in naïve rats (1.8 ± 0.1 *vs.* 1.0 ± 0.1) (Fig. 5P). Ro61-8048 decreased the NOS2 protein levels in the DRG after CCI from 1.8 ± 0.1 to 1.1 ± 0.1 (Fig. 5P).

3.2.4. The influence of repeated i.t. administration of Ro61-8048 or JM6 on the effect of a single dose of morphine on day 7 after CCI

Behavioral tests were conducted 30 min (von Frey test) and 35 min (cold plate test) after *i.t.* administration of Ro61-8048 (10 μg), JM6 (10 μg) or vehicle (DMSO) and were repeated 30 min (von Frey test) and 35 min (cold plate test) after a single *i.t.* injection of morphine (10 μg). Repeated treatment with Ro61-8048 significantly attenuated mechanical allodynia from 14.2 ± 1.0 g to 21.1 ± 0.9 g (Fig. 6A) and cold hyperalgesia from 10.4 ± 0.7 s to 24.0 ± 0.9 s (Fig. 6B). Ro61-8048 enhanced the response to morphine, as demonstrated by the results on the von Frey test

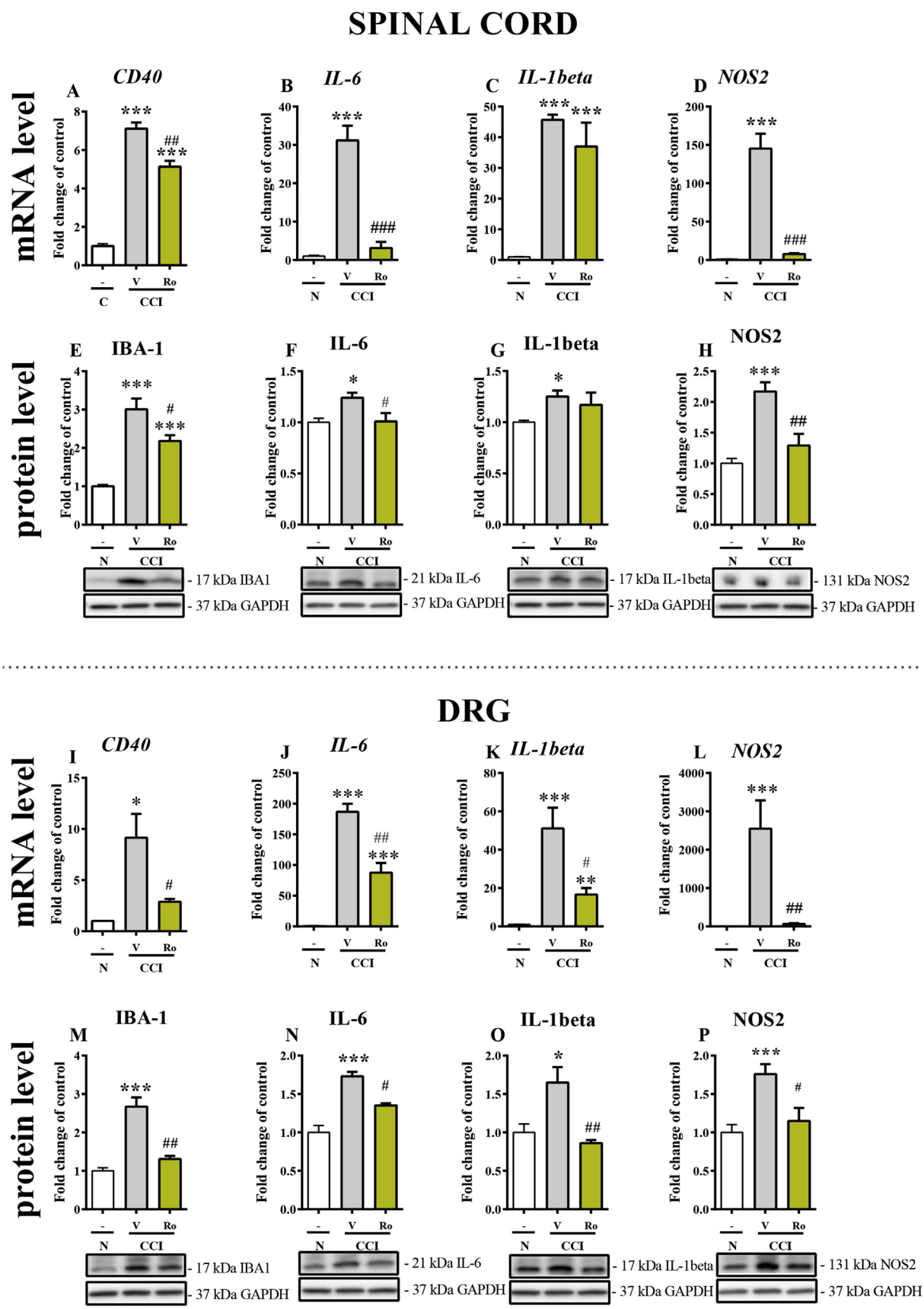

Fig. 5. The effects of repeated administration of Ro61-8048 on the mRNA and protein levels of *CD40*, *IBA-1* (A, E, I, M), *IL-6* (B, F, J, N), *IL-1beta* (C, G, K, O), *NOS2* (D, H, L, P) in the spinal cord and the DRG on day 7 after CCI. The data are shown as the mean fold-changes in expression relative to the control (naïve group) levels ± SEM (4–9 samples for each group). Inter-group differences were analyzed via one-way ANOVA followed by Bonferroni's test for multiple comparisons. *p < 0.05, **p < 0.01 and ***p < 0.001 indicate differences compared to the naïve group; #p < 0.05, ##p < 0.01 and ###p < 0.001 indicate differences compared to the V-treated CCI-exposed group. Abbreviations: N (naïve group); V–CCI (DMSO-treated CCI-exposed group); Ro (Ro61-8048-treated CCI-exposed group).

(20.0 ± 0.6 g *vs.* 25.2 ± 0.7 g, Fig. 6A) and the cold plate test (18.1 ± 2.3 s *vs.* 29.4 ± 0.3 s, Fig. 6B). Similarly, repeated administration of JM6 attenuated mechanical allodynia from 14.2 ± 1.0 g to 20.1 ± 0.6 g (Fig. 6A) and cold hyperalgesia from 10.4 ± 0.7 s to 23.5 ± 0.6 s (Fig. 6B). Furthermore, JM6 enhanced the response to morphine, as demonstrated by the results on the von Frey test (20.0 ± 0.6 g *vs.* 25.0 ± 0.3 g) and the cold plate test (18.1 ± 2.3 s *vs.* 28.5 ± 1.0 s) (Fig. 6A and B).

4. Discussion

Our results showed that pharmacological inhibition of Kmo diminished the symptoms of neuropathic pain and enhanced the effectiveness of morphine in a neuropathic pain model. We observed reductions in the *Kmo* mRNA levels in the spinal cord and the DRG, as well as decreases in pain symptoms, after chronic *i.p.* or *i.t.* administration of minocycline. Moreover, treatment with a Kmo inhibitor (Ro61-6048 or JM6) reduced allodynia and hyperalgesia in CCI-treated rats to a greater extent than treatment with minocycline. Our biochemical studies showed that seven days after sciatic nerve injury, chronic Ro61-6048 administration reduced the *CD-40* mRNA and IBA-1 protein levels in the spinal cord and the DRG. Furthermore, the mRNA and protein levels of pronociceptive factors in the spinal cord (i.e., *IL-6* and *NOS2*) and the DRG (i.e., *IL-1beta, IL-6* and *NOS2*) were reduced after Ro61-6048 treatment. Most importantly, both Kmo inhibitors (Ro61-6048 and JM6) appeared to not only decrease neuropathic pain symptoms but also potentiate the analgesic properties of morphine in a neuropathic pain model.

The molecular mechanisms underlying neuropathy are continuously under investigation to create new opportunities to attenuate neuropathic pain. One drug that exerts beneficial effects against neuropathic pain development is minocycline (Ledeboer et al., 2005; Mika et al., 2007, 2010; Ragavendra et al., 2003). Our previous gene profiling studies (Rojewska et al., 2014b) revealed a set of genes that were modulated by minocycline in rats subjected to CCI. As shown in our studies, the levels of 93 out of the 22,500 evaluated transcripts were changed upon sciatic nerve injury; of these, 54 transcripts were not affected by multiple administrations of minocycline, whereas 39 transcripts displayed strong modulation by recurrent minocycline treatment (Rojewska et al., 2014b). This experiment attracted our attention to *Kmo,* which showed increased expression in association with neuropathy and was decreased in the spinal cord following *i.p.* administration of minocycline (Rojewska et al., 2014b). In the present study, based on qRT-PCR, not only *i.p.* but also *i.t.* administration of minocycline reduced the *Kmo* mRNA levels in the spinal cord and the DRG. Kmo inhibition may be one therapeutically relevant method of protecting injured neurons from further neurotoxicity. However, to our knowledge, the effect of Kmo inhibition on neuronal survival has not been studied under conditions of neuropathic pain. Kmo is an enzyme that plays an important role in the kynurenine pathway (Giorgini et al., 2013); the role of Kmo in neuropathy was not previously considered. Studies of neurodegenerative processes revealed that overexpression of Kmo enhances the production of QUIN, which exerts cytotoxic effects (Behan and Stone, 2000; Campbell et al., 2014; Schwarcz et al., 2012). Reduced Kmo activity promotes the production of kynurenic acid (KYNA), which displays neuroprotective properties. Conversely, Röver et al. (1997) and Vasquez et al. (2000) suggested that QUIN is an agonist of NMDA receptors and, therefore, is neurotoxic. Moreover, Saito et al. (1993) and Reinhard et al. (1994) showed that the cerebral QUIN concentrations are dramatically increased under pathological conditions and that this increase is accompanied by brain inflammation. Based on formalin tests, *i.t.* administration of KYNA produced dose-dependent analgesic effects in rats (Kristensen et al., 1993; Chapman and Dickenson, 1995; Ohshiro et al., 2008) and mice (Nasstrom et al., 1992). The results of many studies confirmed that Kmo inhibitors display neuroprotective properties (Carpenedo et al., 2002; Moroni et al., 2003). Inhibiting Kmo reduces the levels of toxic metabolites of the kynurenine pathway (3-HKA and QUIN), thus preventing neuronal damage via both inflammatory and neurological processes (Chiarugi et al., 2001). Some authors have previously shown that in the R6/2 genetic mouse model of Huntington's disease, peripheral blockade of Kmo reduced the loss of synapses and the activation of microglia while improving survival (Zwilling et al., 2011). Our studies were the first to show that sciatic nerve ligation led to increased *Kmo* mRNA levels; this increase was prevented by minocycline treatment. Thus, Kmo inhibition under conditions of neuropathy may be one strategy to interrupt injury-induced neurotoxicity, which ultimately leads to the development of neuropathic pain. Administering Kmo inhibitors may protect neurons from the spread of neurodegeneration and may serve as a highly therapeutically relevant treatment in the future. Previous studies have confirmed that Ro61-8048 displays neuroprotective activity in animal models of cerebral hypoxia (Röver et al., 1997; Moroni et al., 2005) and dyskinesia (Gregoire et al., 2008), in Huntington's and Alzheimer's diseases (Chin et al., 2005), and following cerebral ischemia (Cozzi et al., 1999). Interestingly, our results suggest that in neuropathic pain, even a single injection of Ro61-8048 or JM6 decreased allodynia and hyperalgesia; this finding confirmed the important role of Kmo in the kynurenine pathway. Interestingly, we also found that Ro61-8048 potentiated the analgesic properties of morphine. In our opinion, Ro61-8048, which is already used to treat neurodegenerative diseases in humans (Campbell et al., 2014), may be a promising drug for the treatment of neuropathic pain.

In 2011, Zwilling et al. published a report regarding the use of JM6 (an oral pro-drug of Ro61-8048), a novel Kmo inhibitor that displays similar activity to Ro61-8048. Experiments conducted in a murine model of Huntington's disease (Zwilling et al., 2011) revealed increased microglial activation (Simmons et al., 2007), which was ameliorated by JM6 administration. As shown in recent reports, administration of JM6 also reduced microglial activation and neuronal damage in APPtg mice, a model of Alzheimer's disease (Chin et al., 2005). Moreover, in an experimental cerebral hypoxia model, Moroni et al. (2005) demonstrated that Kmo inhibitors reduced pyramidal cell damage, probably by inhibiting the synthesis of 3-HK and QUIN. Zwilling et al. (2011) proposed that KMO acts as a mediator between the nervous system and the

Table 1
The effect of a single intrathecal administration of a kynurenine 3-monooxygenase (Kmo) inhibitor (Ro61-8048 or JM6) at a dose ranging from 10 to 120 μg on allodynia and hyperalgesia on day 7 after CCI. The results are presented as the means ± SEM (6–14 rats per group). The inter-group differences were analyzed via one-way ANOVA followed by Bonferroni's test for multiple comparisons. $^{\#\#}p < 0.01$ and $^{\#\#\#}p < 0.001$ indicate differences compared to the vehicle-treated CCI-exposed rats. Abbreviations: V, vehicle; Ro, Ro61-8048; JM6, prodrug for Ro-61-8048.

Treatment	Von Frey	Cold plate
Vehicle	13.8 ± 0.8	10.5 ± 1.1
Ro61-8048 [μg/5 μl; *i.t.*]		
10	15.9 ± 1.3	8.5 ± 1.8
20	19.7 ± 1.2$^{\#\#\#}$	16.9 ± 0.9$^{\#\#\#}$
40	18.2 ± 0.8$^{\#\#}$	16.50 ± 3.1$^{\#\#\#}$
80	19.1 ± 1.0$^{\#\#\#}$	16.8 ± 2.4$^{\#\#\#}$
120	21.6 ± 1.4$^{\#\#\#}$	22.7 ± 1.8$^{\#\#\#}$
JM6 [μg/5 μl; *i.t.*]		
10	14.6 ± 1.0	13.9 ± 1.8
20	14.0 ± 1.0	16.3 ± 0.7
40	17.3 ± 0.9$^{\#\#}$	18.3 ± 2.2$^{\#\#}$
80	19.6 ± 1.4$^{\#\#}$	18.8 ± 1.9$^{\#\#}$
120	20.0 ± 0.9$^{\#\#}$	20.6 ± 1.9$^{\#\#\#}$

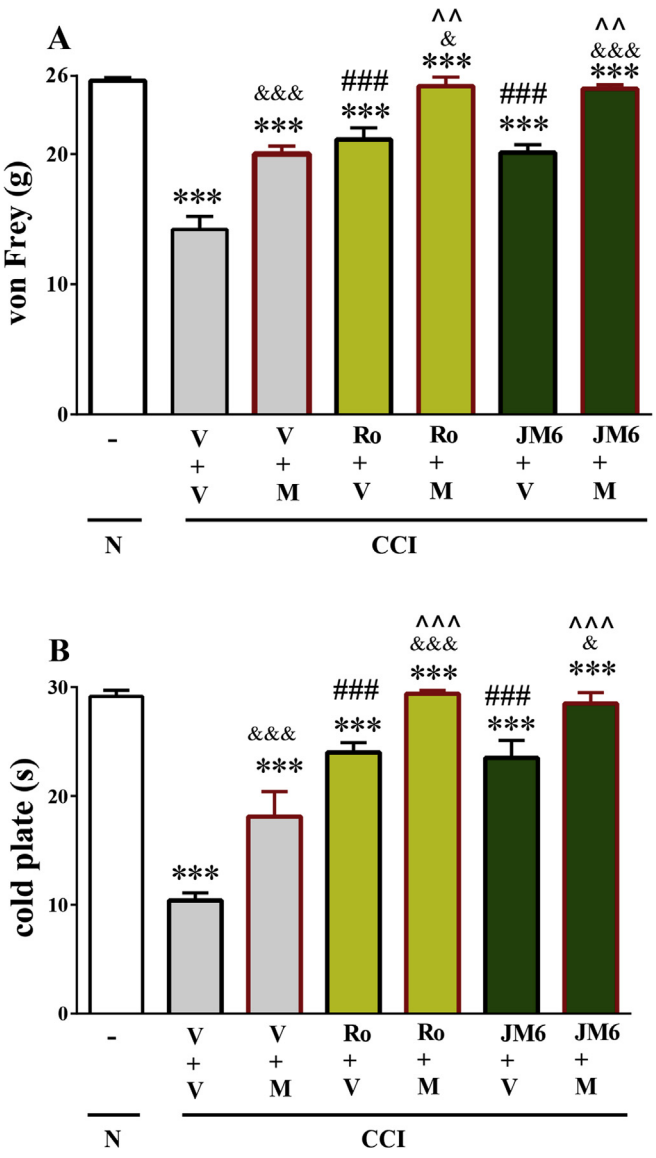

Fig. 6. The effect of Ro61-8048 or JM6 on the analgesic effects of morphine on day 7 after CCI. Ro61-8048 or JM6 (10 μg, *i.t.*) was repeatedly administered to rats subjected to CCI. Rats treated with vehicle, Ro61-8048 or JM6 received a single *i.t.* injection of morphine (M, 10 μg). Behavioral tests were conducted 30 min (von Frey test; A) and 35 min (cold plate test; B) after vehicle, Ro61-8048 or JM6 administration and were repeated 30 min (von Frey test; A) and 35 min (cold plate test; B) after a single morphine injection. The data are presented as the means ± SEM (6–14 rats per group). Inter-group differences were analyzed via one-way ANOVA followed by Bonferroni's test for multiple comparisons. ***$p < 0.001$ indicates a difference compared to the naïve group; ###$p < 0.001$ indicates a difference compared to the V-treated CCI-exposed group; ^^$p < 0.01$ and ^^^$p < 0.001$ indicate differences compared to the morphine-treated CCI-exposed group; &$p < 0.05$ and &&&$p < 0.001$ indicate a significant difference between the Ro61-8048- or JM-6-treated CCI-exposed group and the morphine-treated CCI-exposed group.

immune system, and this suggestion is in agreement with our present results.

In 2006, Ryu et al. studied the role of Kmo in a model of Huntington's disease induced via the administration of QUIN to the striatum; this process activated microglia and increased the expression of pronociceptive factors, such as *IL-1beta*, *IL-6*, *TNFα*, *COX-2* and *NOS2*. In our experiments, we showed that on day 7 after CCI, Ro61-8048 administration reduced the mRNA levels of *CD-40* and of proinflammatory factors such as *IL-6* and *NOS2* in the spinal cord. Based on Western blot, Ro61-8048 diminished the protein levels of IBA-1, IL-6, IL-1beta and NOS2 in the spinal cord. Additionally, Ro61-8048 injection decreased the protein levels of IL-1beta in the DRG. Other authors also reported that QUIN enhanced microglial activation and cytokine production (Croitoru-Lamoury et al., 2003; Guillemin, 2003). Ryu et al. (2006) demonstrated that minocycline suppresses the QUIN-induced activation of microglia and astroglia and expression of the pronociceptive factors COX-2 and NOS2. However, emerging evidence indicates that the Kmo branch of the pathway may be induced by proinflammatory stimuli. In 1997, Heyes et al. demonstrated that Kmo enzyme activity was increased in colonies of macrophages stimulated by IFN-γ. In our primary culture studies of glial cells, we showed that Kmo mRNA expression was strongly upregulated by LPS stimulation in microglia but not astroglia. Moreover, minocycline decreased the LPS-induced enhancement of Kmo expression.

We previously reported (Rojewska et al., 2014b) that after CCI, the gene expression of T-cell (*Cd3g, Cd3e, Cd3d, Cd4,* and *Cd8*), B-cell (*Cd19*) and NK cell (*Cd335*) markers in the spinal cord was unchanged; however, *Cd40* was highly upregulated, and its expression was decreased by minocycline, similar to the effects of minocycline on *Kmo*. Our primary cell culture experiments confirmed that Kmo is expressed in microglia and that *Kmo* is highly upregulated after LPS stimulation. Based on biochemical studies of the spinal cord and previously described data, we reasoned that minocycline reverses LPS-induced microglial activation and decreases Kmo mRNA expression in primary microglial cells. Thus, we hypothesized that under conditions of neuropathic pain, the primary source of Kmo is microglia.

Injury-induced activation of neurodegenerative processes may cause the well-known phenomenon of diminishing efficacy of morphine against neuropathic pain (McQuay, 2002; Porreca et al., 1998). The mechanisms underlying the decreasing analgesic potency of morphine against neuropathic pain have been intensively studied (Mika, 2008; Ossipov et al., 1995; Porreca et al., 1998; Przewlocki and Przewlocka, 2005; Speth et al., 2002). One hypothesis indicates that the disturbed balance between algesic and analgesic factor production by glial cells, especially microglia, might be responsible for the decreasing effectiveness of morphine under conditions of neuropathic pain (Raghavendra et al., 2002, 2003). Researchers showed that IL-1beta and IL-6 produced by microglia had opposing effects on morphine efficacy (Johnston and Westbrook, 2005; Raghavendra et al., 2002, 2003). These results are in agreement with our results showing that microglial inhibitors enhanced the efficacy of morphine against neuropathic pain. Further evidence has shown that inhibiting glial activation improved the efficacy of opioids, which are used in clinical settings for the treatment of neuropathic pain. In our present experiments, we showed that Ro61-6048 reduced Kmo gene expression and microglial activation in the spinal cord and decreased the levels of pronociceptive factors in both the spinal cord (*IL-6* and *NOS2*) and the DRG (*IL-1beta*, *IL-6* and *NOS2*). Therefore, Kmo inhibition may serve as a new strategy to potentiate the analgesic properties of morphine in a similar manner to minocycline (Mika et al., 2007).

5. Conclusion

We observed that pharmacological inhibition of Kmo decreased neuropathic pain. Kmo inhibitors reduced the mRNA expression of *CD40* and concurrently reduced the levels of the pronociceptive factors *IL-1beta*, *IL-6* and *NOS2* in the spinal cord and/or the DRG. Furthermore, we demonstrated that Ro61-6048 decreased the protein levels of IBA-1, IL-6 and NOS2 in the spinal cord as well as IBA-1, IL-6, IL-1beta and NOS2 in the DRG. Most importantly, two Kmo inhibitors (i.e., Ro61-6048 and JM6) potentiated the analgesic properties of morphine under conditions of neuropathic pain.

Therefore, inhibiting Kmo may decrease the negative effects of nerve damage, thus enhancing the effects of analgesics and consequently improving neuropathic pain therapy. Our results are supported by preclinical evidence that administering Kmo inhibitors counteracted the effects of neuroinflammation in various neurodegenerative diseases (Campbell et al., 2014; Wilson et al., 2014). Therefore, our results appear to be promising for the development of future neuropathic pain treatments.

Conflicts of interest

The authors have no conflicts of interest to declare.

Acknowledgments

This work was supported by the National Science Centre, Poland grant Harmonia 5 2013/10/M/NZ4/00261 and by Institute of Pharmacology statutory funds.

Rojewska received a scholarship from the START, which is sponsored by the Foundation of Polish Science, Poland. Piotrowska received a scholarship from the KNOW, which is sponsored by the Ministry of Science and Higher Education, Poland.

References

Behan, W.M., Stone, T.W., 2000. Role of kynurenines in the neurotoxic actions of kainic acid. Br. J. Pharmacol. 129, 1764–1770.
Bennett, G.J., Xie, Y.K., 1988. A peripheral mononeuropathy in rat that produces disorders of pain sensation like those seen in man. Pain 33, 87–107.
Campbell, B.M., Charych, E., Lee, A.W., Möller, T., 2014. Kynurenines in CNS disease: regulation by inflammatory cytokines. Front. Neurosci. 8, 12.
Carpenedo, R., Meli, E., Peruginelli, F., Pellegrini-Giampietro, D.E., Moroni, F., 2002. Kynurenine 3-mono-oxygenase inhibitors attenuate post-ischemic neuronal death in organotypic hippocampal slice cultures. J. Neurochem. 82, 1465–1471.
Chapman, V., Dickenson, A.H., 1995. Time-related roles of excitatory amino acid receptors during persistent noxiously evoked responses of rat dorsal horn neurones. Brain Res. 703, 45–50.
Chiarugi, A., Cozzi, A., Ballerini, C., Massacesi, L., Moroni, F., 2001. Kynurenine 3-mono-oxygenase activity and neurotoxic kynurenine metabolites increase in the spinal cord of rats with experimental allergic encephalomyelitis. Neuroscience 102, 687–695.
Chin, J., Palop, J.J., Puolivali, J., Massaro, C., Bien-Ly, N., Gerstein, H., Scearce-Levie, K., Masliah, E., Mucke, L., 2005. Fyn kinase induces synaptic and cognitive impairments in a transgenic mouse model of Alzheimer's disease. J. Neurosci. 25, 9694–9703.
Chomczynski, P., Sacchi, N., 1987. Single-step method of RNA isolation by acid guanidinium thiocyanate-phenol-chloroform extraction. Anal. Biochem. 162, 156–159.
Collins, S., Sigtermans, M.J., Dahan, A., Zuurmond, W.W., Perez, R.S., 2010. NMDA receptor antagonists for the treatment of neuropathic pain. Pain Med. 11, 1726–1742.
Cozzi, A., Carpenedo, R., Moroni, F., 1999. Kynurenine hydroxylase inhibitors reduce ischemic brain damage: studies with (m-nitrobenzoyl)-alanine (mNBA) and 3,4-dimethoxy-[-N-4-(nitrophenyl)thiazol-2yl]-benzenesulfonamide (Ro61-8048) in models of focal or global brain ischemia. J. Cereb. Blood Flow. Metab. 19, 771–777.
Croitoru-Lamoury, J., Guillemin, G.J., Dormont, D., Brew, B.J., 2003. Quinolinic acid up-regulates chemokine production and chemokine receptor expression in astrocytes. Adv. Exp. Med. Biol. 527, 37–45.
Giorgini, F., Huang, S.Y., Sathyasaikumar, K.V., Notarangelo, F.M., Thomas, M.A., Tararina, M., Wu, H.Q., Schwarcz, R., Muchowski, P.J., 2013. Targeted deletion of kynurenine 3-monooxygenase in mice: a new tool for studying kynurenine pathway metabolism in periphery and brain. J. Biol. Chem. 20, 36554–36566.
Gregoire, L., Rassoulpour, A., Guidetti, P., Samadi, P., Bedard, P.J., Izzo, E., Schwarcz, R., Di Paolo, T., 2008. Prolonged kynurenine 3-hydroxylase inhibition reduces development of levodopa-induced dyskinesias in parkinsonian monkeys. Behav. Brain Res. 186, 161–167.
Guillemin, G.J., Smith, D.G., Smythe, G.A., Armati, P.J., Brew, B.J., 2003. Expression of the kynurenine pathway enzymes in human microglia and macrophages. Adv. Exp. Med. Biol. 527, 105–112.
Heyes, M.P., Chen, C.Y., Major, E.O., Saito, K., 1997. Different kynurenine pathway enzymes limit quinolinic acid formation by various human cell types. Biochem. J. 326, 351–356.
Johnston, I.N., Westbrook, R.F., 2005. Inhibition of morphine analgesia by LPS: role of opioid and NMDA receptors and spinal glia. Behav. Brain Res. 156, 75–83.
Kristensen, J.D., Post, C., Gordh Jr., T., Svensson, B.A., 1993. Spinal cord morphology and antinociception after chronic intrathecal administration of excitatory amino acid antagonists in the rat. Pain 54, 309–316.
Ledeboer, A., Sloane, E.M., Milligan, E.D., Frank, M.G., Mahony, J.H., Maier, S.F., Watkins, L.R., 2005. Minocycline attenuates mechanical allodynia and proinflammatory cytokine expression in rat models of pain facilitation. Pain 115, 71–83.
Makuch, W., Mika, J., Rojewska, E., Zychowska, M., Przewlocka, B., 2013. Effects of selective and non-selective inhibitors of nitric oxide synthase on morphine- and endomorphin-1-induced analgesia in acute and neuropathic pain in rats. Neuropharmacology 75, 445–457.
McQuay, H.J., 2002. Neuropathic pain: evidence matters. Eur. J. Pain 6, 11–18.
Mika, J., 2008. Modulation of microglia can attenuate neuropathic pain symptoms and enhance morphine effectiveness. Pharmacol. Rep. 60, 297–307.
Mika, J., Osikowicz, M., Makuch, W., Przewlocka, B., 2007. Minocycline and pentoxifylline attenuate allodynia and hyperalgesia and potentiate the effects of morphine in rat and mouse models of neuropathic pain. Eur. J. Pharmacol. 560, 142–149.
Mika, J., Korostynski, M., Kaminska, D., Wawrzczak-Bargiela, A., Osikowicz, M., Makuch, W., Przewlocki, R., Przewlocka, B., 2008. Interleukin-1 alpha has antiallodynic and antihyperalgesic activities in a rat neuropathic pain model. Pain 138, 587–597.
Mika, J., Osikowicz, M., Rojewska, E., Korostynski, M., Wawrzczak-Bargiela, A., Przewlocki, R., Przewlocka, B., 2009. Differential activation of spinal microglial and astroglial cells in a mouse model of peripheral neuropathic pain. Eur. J. Pharmacol. 623, 65–72.
Mika, J., Rojewska, E., Makuch, W., Przewlocka, B., 2010. Minocycline reduces the injury-induced expression of prodynorphin and pronociceptin in the dorsal root ganglion in a rat model of neuropathic pain. Neuroscience 165, 1420–1428.
Mika, J., Zychowska, M., Popiolek-Barczyk, K., Rojewska, E., Przewlocka, B., 2013. Importance of glial activation in neuropathic pain. Eur. J. Pharmacol. 716, 106–119.
Milligan, E.D., Watkins, L.R., 2009. Pathological and protective roles of glia in chronic pain. Nat. Rev. Neurosci. 10, 23–36.
Moroni, F., Carpenedo, R., Cozzi, A., Meli, E., Chiarugi, A., Pellegrini-Giampietro, D.E., 2003. Studies on the neuroprotective action of kynurenine mono-oxygenase inhibitors in post-ischemic brain damage. Adv. Exp. Med. Biol. 527, 127–136.
Moroni, F., Cozzi, A., Carpendo, R., Cipriani, G., Veneroni, O., Izzo, E., 2005. Kynurenine3-mono-oxygenase inhibitors reduce glutamate concentration in the extracellular spaces of the basal ganglia but not in those of the cortex or hippocampus. Neuropharmacology 48, 788–795.
Näsström, J., Karlsson, U., Post, C., 1992. Antinociceptive actions of different classes of excitatory amino acid receptor antagonists in mice. Eur. J. Pharmacol. 212, 21–29.
Ohshiro, H., Tonai-Kachi, H., Ichikawa, K., 2008. GPR35 is a functional receptor in rat dorsal root ganglion neurons. Biochem. Biophys. Res. Commun. 365, 344–348.
Ossipov, M.H., Lopez, Y., Nichols, M.L., Bian, D., Porreca, F., 1995. The loss of antinociceptive efficacy of spinal morphine in rats with nerve ligation injury is prevented by reducing spinal afferent drive. Neurosci. Lett. 199, 87–90.
Porreca, F., Tang, Q.B., Bian, D., Riedl, M., Elde, R., Lai, J., 1998. Spinal opioid mu receptor expression in lumbar spinal cord of rats following nerve injury. Brain Res. 795, 197–203.
Przewlocki, R., Przewlocka, B., 2005. Opioids in neuropathic pain. Curr. Pharm. Des. 11, 3013–3025.
Raghavendra, V., Rutkowski, M.D., DeLeo, J.A., 2002. The role of spinal neuroimmune activation in morphine tolerance/hyperalgesia in neuropathic and shamoperated rats. J. Neurosci. 22, 9980–9989.
Raghavendra, V., Tanga, F., DeLeo, J.A., 2003. Inhibition of microglial activation attenuates the development but not existing hypersensitivity in a rat model of neuropathy. J. Pharmacol. Exp. Ther. 306, 624–630.
Reinhard Jr., J.F., Erickson, J.B., Flanagan, E.M., 1994. Quinolinic acid in neurological disease: opportunities for novel drug discovery. Adv. Pharmacol. 30, 85–125.
Rojewska, E., Makuch, W., Przewlocka, B., Mika, J., 2014a. Minocycline prevents dynorphin-induced neurotoxicity during neuropathic pain in rats. Neuropharmacology 86, 301–310.
Rojewska, E., Korostynski, M., Przewlocki, R., Przewlocka, B., Mika, J., 2014b. Expression profiling of genes modulated by minocycline in a rat model of neuropathic pain. Mol. Pain 10, 47.
Rojewska, E., Popiolek-Barczyk, K., Jurga, A.M., Makuch, W., Przewlocka, B., Mika, J., 2014c. Involvement of pro- and antinociceptive factors in minocycline analgesia in rat neuropathic pain model. J. Neuroimmunol. 277, 57–66.
Röver, S., Cesura, A.M., Huguenin, P., Kettler, R., Szente, A., 1997. Synthesis and biochemical evaluation of N-(4-phenylthiazol-2-yl) benzenesulfonamides as high-affinity inhibitors of kynurenine 3-hydroxylase. J. Med. Chem. 40, 4378–4385.
Ryu, J.K., Choi, H.B., McLarnon, J.G., 2006. Combined minocycline plus pyruvate treatment enhances effects of each agent to inhibit inflammation, oxidative damage, and neuronal loss in an excitotoxic animal model of Huntington's disease. Neuroscience 141, 1835–1848.
Saito, K., Nowak, T.S., Markey, S.P., Heyes, M.P., 1993. Mechanism of delayed increases in Kynurenine pathway metabolism in damaged brain regions following transient cerebral ischemia. J. Neurochem. 60, 180–192.
Schwarcz, R., Bruno, J.P., Muchowski, P.J., Wu, H.Q., 2012. Kynurenines in the mammalian brain: when physiology meets pathology. Nat. Rev. Neurosci. 13, 465–477.
Simmons, D.A., Casale, M., Alcon, B., Pham, N., Narayan, N., Lynch, G., 2007. Ferritin accumulation in dystrophic microglia is an early event in the development of

Huntington's disease. Glia 55, 1074–1084.
Speth, C., Dierich, M.P., Gasque, P., 2002. Neuroinvasion by pathogens: a key role of the complement system. Mol. Immunol. 38, 669–679.
Vazquez, S., Garner, B., Sheil, M.M., Truscott, R.J., 2000 Jan. Characterisation of the major autoxidation products of 3-hydroxykynurenine under physiological conditions. Free Radic. Res. 32 (1), 11–23.
Wilson, K., Mole, D.J., Binnie, M., Homer, N.Z., Zheng, X., Yard, B.A., Iredale, J.P., Auer, M., Webster, S.P., 2014. Bacterial expression of human kynurenine 3-monooxygenase: solubility, activity, purification. Protein Expr. Purif. 95, 96–103.
Yaksh, T.L., Rudy, T.A., 1976. Chronic catheterization of the spinal subarachnoid space. Physiol. Behav. 17, 1031–1036.
Zawadzka, M., Kaminska, B., 2005. A novel mechanism of FK506-mediated neuroprotection: downregulation of cytokine expression in glial cells. Glia 49, 36–51.
Zimmermann, M., 1983. Ethical guidelines for investigations of experimental pain in conscious animals. Pain 16, 109–110.
Zwilling, D., Huang, S.Y., Sathyasaikumar, K.V., Notarangelo, F.M., Guidetti, P., Wu, H.Q., Lee, J., Truong, J., Andrews-Zwilling, Y., Hsieh, E.W., Louie, J.Y., Wu, T., Scearce-Levie, K., Patrick, C., Adame, A., Giorgini, F., Moussaoui, S., Laue, G., Rassoulpour, A., Flik, G., Huang, Y., Muchowski, J.M., Masliah, E., Schwarcz, R., Muchowski, P.J., 2011. Kynurenine 3-monooxygenase inhibition in blood ameliorates neurodegeneration. Cell 145, 863–874.